



TREE CANOPY COVER ESTIMATION BY MEANS OF REMOTELY SENSED DATA FOR LARGE GEOGRAPHICAL AREAS: OVERVIEW, AVAILABLE DATA, AND PROPOSAL

Colaninno, Nicola ^{1*}; Eldesoky, Ahmed Hazem Mahmoud ²; Morello, Eugenio ³

Initial submission: 2019-07-17; **Definitive submission:** 2019-10-21; **Publication:** 2019-12-21

Citation: Colaninno, N. *et al.* (2019). Tree canopy cover estimation by means of remotely sensed data for large geographical areas: overview, available data, and proposal. In *XIII CTV 2019 Proceedings: XIII International Conference on Virtual City and Territory: "Challenges and paradigms of the contemporary city"*: UPC, Barcelona, October 2-4, 2019. Barcelona: CPSV, 2019, p. 8650. E-ISSN 2604-6512. DOI <http://dx.doi.org/10.5821/ctv.8650>

Abstract

Climate change and global warming requires a strong boost to sustainable growth strategies. In particular, urban green management and planning is becoming a crucial and at the same time critical aspect. Therefore, urban green requires being accurately mapped, quantified and monitored over time. In this study we propose a cost-effective but reliable approach for the automatic classification and quantification of the tree canopy cover over extended geographical areas. The classification can also be used for estimating the number of trees, based on land use land cover (LULC) and the corresponding planting layout. The case study application is the Metropolitan City of Milan. Data used for classifying the tree canopy are based on high-resolution satellite imagery provided by the PlanetScope constellation. Based on the latter information, the work relies on the use of radiometric Vegetation Indices (VIs) to quantify the tree canopy. However, because the use of VIs can cause mixing of different types of vegetation, such as tree and grass, we used a stack of multi-temporal data from PlanetScope to retrieve per-pixel statistics for Red band and Normalized Difference Vegetation Index (NDVI). The hypothesis here is that during spring-summer season tree canopy provides less variability than grass and/or agricultural fields. The approach provides an improved vegetation index capable of separating potential canopy-tree from other vegetation types. The result of the accuracy assessment shows an overall accuracy of 78.33% and 71.5% for the whole Metropolitan City of Milan and the City of Milan respectively.

Keywords: tree canopy; urban forestation; remote sensing; climate change

1. Introduction

Climate change and global warming require urgent solutions towards a sustainable growth. As part of the global policy framework and commitment recently promoted by the United Nations through the 2030 Agenda, the Paris Agreement and the New Urban Agenda, cities are expected to play a key role. Actually, while during the past decades urban sustainability was mostly related to the dualism compact city versus sprawl and the rhetoric of urban infilling, more recently, the promotion of urban greening strategies shifted attention to the dualism building density versus vegetation density with a focus on boosting soil permeability and urban green management (Haaland & van den Bosch, 2015). In fact, green infrastructure can favour a sustainable growth and provides benefits in terms of climate mitigation and air quality improvement. This evidence has been extensively demonstrated (Bowler, Buyung-Ali, Knight, & Pullin, 2010). Nonetheless, urban green requires being accurately quantified and monitored. In order to face such a matter, important efforts are now being put in place by cities globally.

¹ Laboratorio di Simulazione Urbana Fausto Curti, Dept. Architecture and Urban Studies, Politecnico di Milano, <https://orcid.org/0000-0003-4428-639X>; ² Università IUAV di Venezia, <https://orcid.org/0000-0002-6381-8956>; ³ Laboratorio di Simulazione Urbana Fausto Curti, Dept. Architecture and Urban Studies, Politecnico di Milano, <https://orcid.org/0000-0003-2382-6123>. * Contact e-mail: nicola.colaninno@polimi.it



The Million Tree initiative, for instance, aimed at increasing the urban forest to reduce carbon dioxide and the effects of heat waves (McPherson & Kendall, 2014), involves different cities like Los Angeles, Denver, New York, Shanghai, London and Ontario. The Treepedia project measures the canopy cover at the street level for several cities globally, including Boston, New York, London, Paris, Turin and Sydney (Ratti, Seiferling, Li, Ghaeli, & So, n.d.). Besides, the European Space Agency in collaboration with the Greater London Authority promoted the mapping of the tree canopy cover for the Greater London area (Breadboard Labs, 2018), carried out under the Curio Canopy project (ESA, n.d.). In line with these above-mentioned projects, Milan has recently launched an ambitious forestation project that aims at planting about 3 million trees for the whole metropolitan territory during the next 10 years.

Assessing tree stock for obtaining a reliable baseline, and for monitoring the progress of planting, remains challenging for most of the urban forestation initiatives. Moreover, quantifying tree canopy in cities stimulates several investigations aimed at measuring the impact of vegetation upon urban climate mitigation and water retention improvement.

In particular, in terms of tree classification, different approaches have been provided, which rely on the use and processing of very-high resolution remotely sensed data. Main remote sensing approaches rely on either active remote sensing, such as radar and Light Detection and Ranging (LiDAR), as well as passive remote sensing based on very-high resolution multispectral imagery, also acquired in stereo mode, including satellites equipped with optical sensors such as GeoEye-1, WorldView, and Pleiades, among others.

Remote sensing applications aimed at measuring tree and building heights require a digital terrain model (DTM) in addition to a digital surface model (DSM) to get information of objects and ground height. In fact, the combination of DTM and DSM allows generating a normalized digital surface model (nDSM), which provides the relative height above ground. The standard procedure for extracting DSM and DTM relies on the use of airborne LiDAR data. However, a number of satellite programs are now employing Very High Resolution (VHR) optical sensors, which provide the ability to capture stereo or even tri-stereo imagery with a ground sample distance below 1 meter (Perko, Raggam, Gutjahr, & Schardt, 2015; Poli & Caravaggi, 2012). According to Perko, et al. (Perko et al., 2015), the question arises if stereo-based DSMs could replace LiDAR data for certain applications, so, they provide qualitative and quantitative evaluations to highly accurate reference LiDAR data to demonstrate the functionality of stereo-based DSMs according to a proposed algorithm for DSM extraction (Perko et al., 2015).

On the other hand, with respect to LiDAR data, and according to Poli and Caravaggi (2012), the availability of multispectral channels in optical stereo images enhance the capabilities for object classification. In particular, it has been reported that, in case of forest, the stereo derived DSM clearly shows a different height with respect to adjacent cultivated areas or grass. Likewise, in urban areas, buildings and transport infrastructure are generally well outlined both in flat and hilly terrains. Moreover, stereo images acquired by satellite VHR optical sensors allow managing large metropolitan areas (Poli & Caravaggi, 2012).

Currently, expert classification algorithms such as rule-based, object-oriented and fuzzy approaches are used for extracting objects from LiDAR data or multispectral imagery. In particular, it is achieved in digital photogrammetry by using 3D information from image matching or DSM/DTM data, spectral, textural and other information sources (Demir, Poli, & Baltsavias,



2008). For instance, buildings and trees are extracted from LiDAR based on filtering algorithms applied to DSM using both raw data as well as interpolated data. Individual tree crowns are detected also by means of watershed segmentation applied to LiDAR data (Chen, Baldocchi, Gong, & Kelly, 2006), or to aerial colour infrared image texture (Vauhkonen et al., 2012). On the other hand, 2D maps are used as prior information for building extraction in LiDAR. However, in order to overcome the limitations of image-based and LiDAR-based techniques, it is of advantage to use a combination of these techniques (Ackermann, 1999; Demir et al., 2008). As reported by Demir, et al. (Demir et al., 2008), Sohn and Dowman (Sohn & Dowman, 2007) used high-resolution multispectral imagery to first identify building regions prior to extract them from LiDAR data, for instance, while Straub (2004) extracts trees by combining infrared imagery and LiDAR data.

Demir, et al. (Demir et al., 2008) have investigated four different approaches based on both image and LiDAR data. The first method combines DSM/DTM with Normalized Different Vegetation Index (NDVI), the second approach is a supervised classification from multispectral imagery then refined with height information from LiDAR, the third method uses voids in LiDAR DTM and NDVI classification, while the last one uses vertical density of the raw DSM LiDAR data (Demir et al., 2008). They report about 96% accuracy by combining the four methods.

Nonetheless, both LiDAR data and very-high resolution stereo images are currently still quite expensive. In addition, for analysis of huge geographical areas, managing such an information is highly consuming in terms of computation time and power. In order to tackle such limitations, we firstly propose a cost-effective but reliable approach for the automatic classification of tree canopy over extended geographical areas.

The approach relies on high-resolution spectral imagery at 3 meters, as provided by the PlanetScope satellite. Multitemporal observations are considered, under the hypothesis that tree canopy provides less variability than grass and/or agricultural fields mostly during spring-summer season. Finally, the classification is then used for quantifying the overall tree canopy area, as well as for estimating the number of trees, based on land use land cover (LULC) and the corresponding planting layout.

2. Study area and data

2.1 Study area

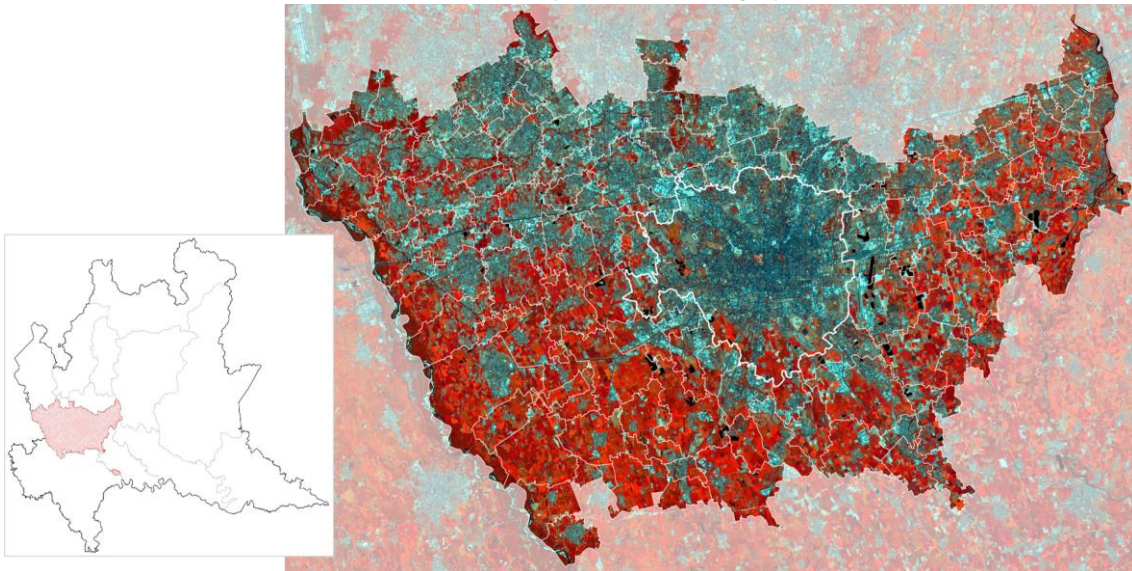
The area under investigation (Figure 1) is the Metropolitan City of Milan (CMM), previously identified as the Province of Milan, which constitutes an administrative ambit, within the Lombardy Region, that covers an area of about 1,600 square kilometres and encompasses a population of over 3 million inhabitants. The CMM was initially defined in 1990, by the reform of local authorities, and later officially recognized in 2014, becoming operative in 2015. The area is made upon an agglomeration of 134 municipalities, including the City of Milan, which is also the administrative capital.

Geographically, the CMM is in central-western Lombardy, along the high Po Valley encompassed by the river Ticino on the west and the river Adda on the east. The territory is structured upon a system of major green areas recognized as protected regional parks due to the high natural-ecological value. Particularly significant, for its dimensions, is the South Milan



Agricultural Park (*Parco Agricolo Sud Milano*), which occupies an area of around 47.000 ha, spanning along a semi-circular area from east to west and covering almost all the southern part of the CMM, including 61 municipalities.

Figure 1. Lombardy Region (left side), and the Metropolitan City of Milan (right side) as viewed by Sentinel-2 imagery



Source: Authors

2.2 Employed data

Data used for classifying the tree canopy is based on high-resolution satellite imagery provided by the PlanetScope constellation. The latter consists of approximately 130 sun-synchronous satellites able to collect land surface coverage, with a daily revisit time, for the entire Earth. PlanetScope imagery is given at different levels of processing. Here we used the PlanetScope Analytic Ortho Scene product (as detailed in Table 1), which relies on surface reflectance (SR) 4-bands multispectral imagery, including blue, green, red, and Near Infrared (NIR), at a spatial resolution of about 3 meters. Nominal scene size is approximately 24 km by 7 km, but varies by altitude (Planet Labs, 2018).

Analytic products, processed at level 3B, rely on calibrated multispectral imagery that have been processed to remove distortions and allow analysts to derive information products for data science and analytics. In particular, ortho-scenes are radiometrically-, sensor-, geometrically- and atmospheric-corrected. Geometrical correction, which uses fine Digital Elevation Models (DEMs) with a post spacing of between 30 and 90 meters, is applied to eliminate the perspective effect on the ground (not on buildings), restoring the geometry of a vertical shot; while radiometric corrections are applied to correct for any sensor artefacts and transformation to at-sensor radiance. Besides, the imagery has been atmospherically corrected to account for atmospheric, surface and spectral conditions and geometry when converting top of atmosphere reflectance to surface reflectance (Planet Labs, 2018).



Table 1. PlanetScope Analytic Ortho Scene Product Specification

Product Attribute	Description
Information Content	
Analytic Bands	3-band multispectral image (red, green, blue) 4-band multispectral image (blue, green, red, near-infrared)
Ground Sample Distance	3.7 m (average at reference altitude 475 km)
Processing	
Pixel Size (orthorectified)	3.125 m
Bit Depth	Analytic (DN): 12-bit Analytic (Radiance - $W\ m^{-2}\ sr^{-1}\ \mu m^{-1}$): 16-bit Analytic SR (Surface Reflectance): 16-bit
Geometric Corrections	Sensor-related effects are corrected using sensor telemetry and a sensor model. Spacecraft-related effects are corrected using attitude telemetry and best available ephemeris data. Orthorectified using GCPs and fine DEMs (30 m to 90 m posting) to <10 m RMSE positional accuracy.
Positional Accuracy	Less than 10 m RMSE
Radiometric Corrections	<ul style="list-style-type: none"> • Conversion to absolute radiometric values based on calibration coefficients • Radiometric values scaled by 100 to reduce quantization error • Calibration coefficients regularly monitored and updated with on-orbit calibration techniques.
Atmospheric Corrections	<ul style="list-style-type: none"> • Conversion to top of atmosphere (TOA) reflectance values using at-sensor radiance and supplied coefficients • Conversion to surface reflectance values using the 6SV2.1 radiative transfer code and MODIS NRT data • Reflectance values scaled by 10,000 to reduce quantization error

Source: Planet imagery product specifications, Planet Labs (2018).

Regarding the land use classification, which has been employed for defining different planting layouts, we used the regional database of the DUSAF project (*Destinazione d'Uso dei Suoli Agricoli e Forestali*), available for all the provinces within the Lombardy Region. The available data is obtained by means of photointerpretation of the orthophotos obtained in 2015 by AGEA (*Agenzia per le erogazioni in agricoltura*) and provided by the Lombardy Region.

The images are detected with two different resolutions, i.e. 50x50 cm in the alpine mountain areas, and 20x20 cm in the lowland and Apennine areas. The recommended operational scale is 1:1,000. The DUSAF relies on a nomenclature divided into 3 main levels consistent with the Corine Land Cover (CLC). In fact, the first level includes the five major categories of coverage (artificial areas, agricultural areas, wooded areas and semi-natural environments, wet areas, water bodies), progressively detailed on the second and third level, consistent with the CLC database. Two additional levels (the fourth and the fifth) provide further attributes of the Lombard territory.

3. Methodology

3.1 An improved vegetation index based on multispectral-multitemporal observation

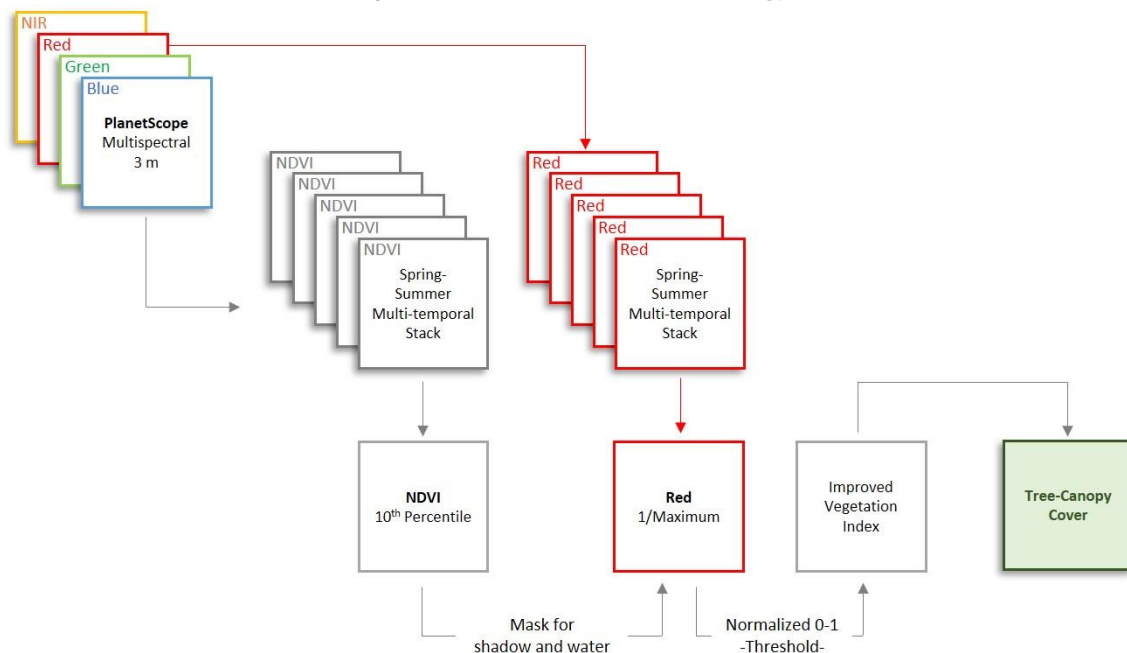
Through remote sensing, vegetation can be estimated from multispectral imagery by means of radiometric Vegetation Indices (VI). Among the VIs, the Normalized Difference Vegetation Index (NDVI) introduced by Rouse, et al. (Rouse, Haas, Deering, Schell, & Harlan, 1974), is among the most explored. However, the NDVI can lack in discriminating grass by trees.

The hypothesis here is that during spring-summer season tree canopy provides less variability than grass and/or agricultural fields. Therefore, based on a stack of multi-temporal multi-spectral images we have investigated per-pixel statistics for both NDVI and spectral bands to get an improved vegetation index.

Actually, it is widely recognized that NDVI provides effective mapping over a wide range of conditions, due to a good balance between the normalized difference formulation, and the use of the highest regions of chlorophyll absorption, and reflectance, within the electromagnetic spectrum. According to the theory behind the formulation of the NDVI, it is known that in any vegetation type, cell structure of the leaves strongly reflects near infrared light (from 0.75 to 1.5 μm), while absorbs the visible light (from 0.4 to 0.75 μm) for use in photosynthesis. Within the visible range, the highest rate of absorption is along the red slice of the spectrum (from 0.6 to 0.75 μm). In general, if there is much more reflected radiation in NIR wavelengths than in visible wavelengths, then the vegetation in that pixel is likely to be dense. Whereas, if there is very little difference in the intensity of visible and NIR wavelengths reflected, then the vegetation is probably sparse and may consist of grassland, tundra, or desert (Weier & Herring, 2000).

Based on such an assumption, we designed a methodology for improving, at a territorial scale, the capability of spectral information for identifying tree canopy by emphasizing the difference among the latter and other types of vegetation. We worked with image statistics applied to a stack of multitemporal observations of NDVI and red band as depicted in Figure 2.

Figure 2. Workflow of the methodology



Source: Authors

Under the hypothesis that during the spring-summer season tree canopy provides less variability than grass and/or agricultural fields, we have selected a set of ten multispectral PlanetScope images ranging from about mid-April to mid-October 2018, as reported in Table 2.

Table 2. Multitemporal dataset of PlanetScope images used for the investigation

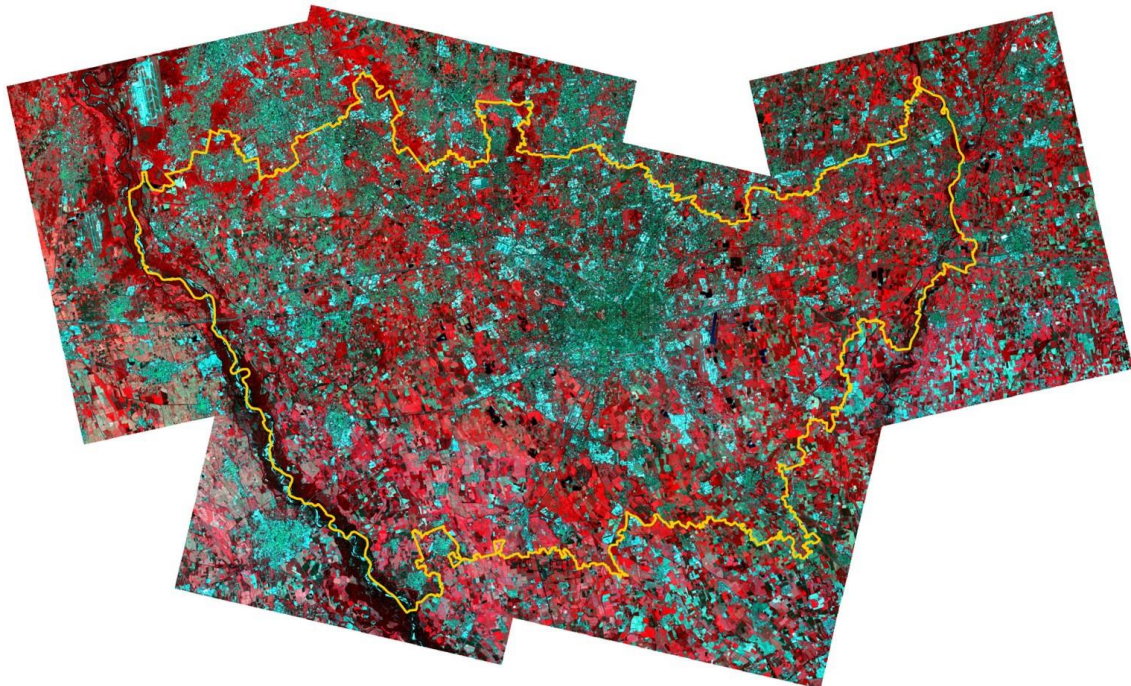
Product	Date	Number of Images
Analytic Bands 4-band multispectral image	1 2018 April 22 (+ April 21)	32 (+4)
	2 2018 April 25 (+April 24)	27 (+12)
	3 2018 June 02	27
	4 2018 June 30 (+June 29)	21 (+11)
	5 2018 July 08	21
	6 2018 August 05 (+August 06)	24 (+8)
	7 2018 August 22 (August 20)	23 (+7)
	8 2018 September 04 (Sept. 05)	29 (+2)
	9 2018 Sept. 24 (Sept. 23, Sept. 26)	16 (+7, +5)
	10 2018 October 23 (Oct. 22, Oct. 24)	25 (+7, +7)

Source: Authors

Since PlanetScope provides nominal scene size of approximately 24 km by 7 km, several images have been downloaded for each date to cover the area under investigation. Also, due to cloud cover, additional images were needed for some dates in order to cover the whole area. For instance, as reported in the previous Table 2, for April the 22nd, we needed to compose the image with further images taken on April 21st.

Then, all the scenes, for each date, have been mosaiced as shown in the sample of Figure 3. In order to get a homogeneous scene, we used a colour balancing algorithm as provided in ENVI to mosaic all the images. Figure 4 provides a sample area used for displaying the results of applying image statistics as depicted in the previous workflow (Figure 2).

Figure 3. PlanetScope images mosaic sample



Source: Authors



Figure 4. **Multispectral image sample area: Natural colour combination (left); Colour-Infrared combination (right)**

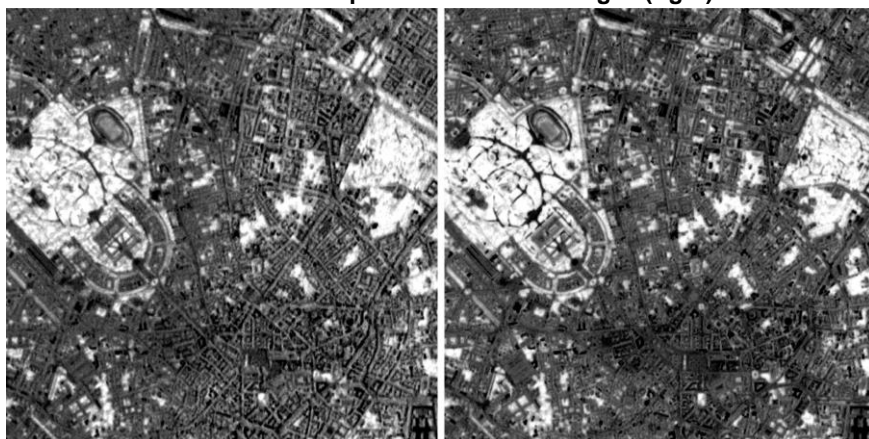


Source: Authors

Once all homogeneous mosaics and the multi-temporal stack for the whole area have been obtained, the NDVI at each temporal stage has been calculated. Hence, the 10th percentile of the multitemporal stack of NDVIs, as well as the maximum of the red bands stack have been computed. If we consider two main typologies of trees, i.e. evergreen and deciduous trees, we can assume that during the spring-summer season both types have a high vegetative vigour. Minimum values of NDVI, retrieved combining multiple observations during this season, theoretically should not affect the detection of trees.

On the other hand, the use of minimum NDVI values enhances the capability of excluding those green areas, such as rural areas, that provide an increased variability through multiple observations during a relative long time period. However, in order to avoid excluding useful information, we used the 10th percentile of the NDVI instead of the minimum, still we get information capable of refining the capability of NDVI to emphasize vegetation with respect to other classes such as shadows in street canyons as shown in Figure 5.

Figure 5. **NDVI sample area: NDVI on October 23rd, 2018 (left); 10th percentile of the NDVI calculated for the multitemporal stack of the images (right)**



Source: Authors

On the other hand, it is demonstrated that green leaves strongly absorb in red band. Hence, maximum value of red band, across a multitemporal stack, emphasizes those green areas with less time variability (during spring-summer) by highlighting those objects that absorb more the red light. Figure 6 shows a red band sample (left) with respect to the maximum red (middle). Maximum red has been reversed to emphasize vegetation in light shades (on the right).

Figure 6. Red band sample area: Red band on October 23rd, 2018 (left); maximum red band (middle); reverse of maximum red band (right)



Source: Authors

Figure 7 shows the improvement of maximum red for discriminating different vegetation types. In the case of the golf course, the maximum of red band (right side) can discriminate among grass and trees or shrubs.

On the other hand, red band strongly absorbs light for shaded areas, which is a critical issue within urban areas. Maximum red band has been normalized from 0 to 1 and a threshold value has been applied, by on-screen interpretation, for selecting potential tree-canopy pixels. Hence, we used the 10th percentile of the NDVI (Figure 7, middle) for masking the maximum of the red band in order to avoid mixing trees with shadows. Moreover, the NDVI is needed for masking water. In fact, the latter is not discriminated through the red band.

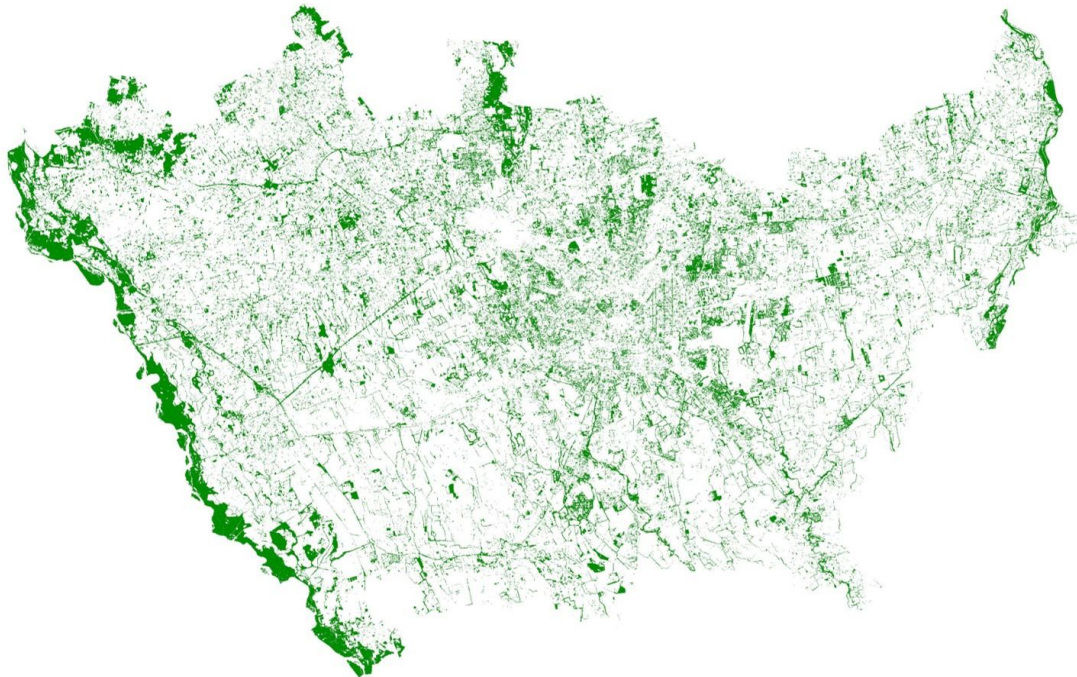
Figure 7. High resolution satellite image sample (left), and comparison among the 10th percentile of NDVI (middle) and maximum red band (right)



Source: Authors

The results, as depicted in Figures 8 and 9, which show the whole area under investigation and some details of the results respectively, have been reviewed and slightly refined on-screen, based on very-high resolution imagery as provided by Google satellite service in QGIS.

Figure 8. Tree-canopy cover for the metropolitan area of Milan at the year 2018



Source: Authors

Figure 9. Details of the tree-canopy cover classification



Source: Authors

3.2 Accuracy assessment

In order to assess the accuracy of the classification, we have used a confusion matrix to compare a randomly selected sample of the results to additional ground truth information. In particular, we have used about 203 points, randomly distributed across the whole Metropolitan City of Milan, by using a sample size calculator², based on equation (1), to determine the minimum points required for conducting the accuracy assessment, based on the size of the input data.

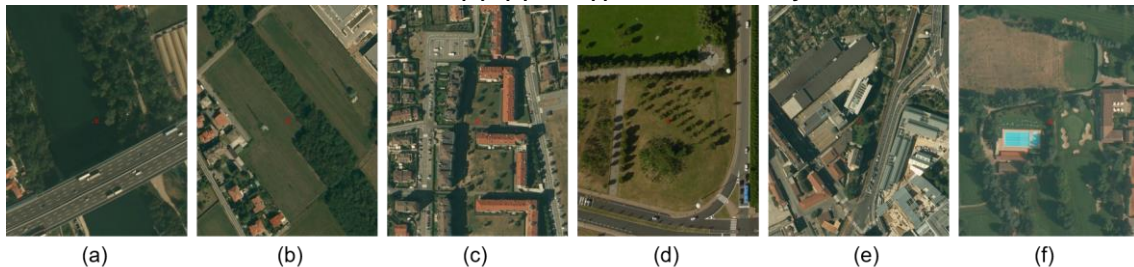
² <http://www.berrie.dds.nl/calcss.htm>

$$n = \frac{N \times Z_{\alpha}^2 p \times q}{d^2 \times (N - 1) + Z_{\alpha}^2 \times p \times q} \quad (1)$$

Where, N is total population number, Z_{α} equals 1.96 squared (the confidence is 95%), p is the expected proportion (in this case 5% = 0.05), q equals $(1 - p)$, and d is a precision percentage (5%). Moreover, in order to assess the quality of the classification over the most urbanized area, which is the most challenging, we have conducted a further accuracy assessment using other 200 randomly distributed points, across the city of Milan.

The result of the accuracy assessment shows an overall accuracy of 78.33% and 71.5% for the whole Metropolitan City of Milan and the city of Milan respectively. Figure 10 shows some examples of accurately classified trees as well as some classification errors.

Figure 10. Samples of the accuracy assessment results, using ground truth points. (a), (b) and (c) refer to misclassification; (d), (e) and (f) show accurately classified trees



Source: Authors

3.3 Tree number estimation based on planting layout

Finally, LULC is used for separating different typologies of green (macro classes), and to assign different planting layouts. Based on this, a rough number of trees can be estimated using a rule of thumb of trunk-to-trunk distance for each land cover type as provided by DUSAF. In order to test the approach, we applied the process to a sample transect.

The DUSAF has been generalized into four classes, i.e. artificial areas, urban green, rural, natural/forest areas. Depending on the latter generalization, different planting layouts have been assigned. Mainly based on an empirical investigation about most common crown dimensions of trees in the City of Milan, we have used 13 meters as distance among trees within the artificial area. While we have reduced the distance to 10 for urban green. We have used 10 meters for agricultural areas, while 6 meters for natural/forest areas. The latter measure is according to the rural development plan of Lombardy Region.

A tool *genregularpntsinpolys* within the Geospatial Modelling Environment (Beyer, 2012), and compatible with ArcMap, was used to generate samples of regularly spaced points within the tree canopy polygons, using the rule of thumbs referred to the assigned planting layout.

Figure 11 shows two samples of the automatic assignment of regularly spaced points within the tree canopy polygons.

Figure 11. Sample of automatic assignment of regularly spaced points within tree canopy polygons



Source: Authors

4. Conclusions

Under the framework of the forestation project, we aimed at establishing a reliable baseline for assessing the current tree canopy in the territory at the year 2018. To achieve this, we made a first exploration based on freely available data, as provided by the satellite PlanetScope, despite evident constraints in terms of spatial resolution and detail. In fact, the result of this study must be intended suitable for an operational scale of 1:12,000.

Actually, a more effective estimation of tree canopy should rely on both very-high resolution multispectral data and the digital surface model (DEM) that provides objects' elevation. However, the high-resolution DEM, which could be obtained by means of LiDAR sensors or stereo-pair satellite images, is still expensive and time-consuming, especially for mapping huge areas. In order to compensate for such a limitation, we explored a cost-effective and replicable approach. On the other hand, the use or radar imagery could be investigated in future developments, as further resource for better discriminating between tree canopy and on-the-ground vegetation at this operational scale.



Acknowledgements: We are highly indebted to Fondazione Falck and F.S. Sistemi Urbani for providing generous funding for carrying out this study. The authors would like to thank the City of Milan and the Metropolitan City of Milan for making data available and for supporting in reviewing the work. We also would like to thank the Planet Team for providing the Planet Application Program Interface: In Space for Life on Earth. San Francisco, CA. <https://api.planet.com>.

Authors' contributions: All authors equally contributed to the idea of the paper and the discussion of its content. Nicola Colaninno is responsible for the ideation of the scientific methodology, the reconstruction of the state of the art, data acquisition and the technical processing of data; Ahmed Eldesoky contributed to the technical processing of the data; Eugenio Morello provided a scientific supervision of the study. The manuscript was intensively revised several times by all authors.

Conflict of Interest: The authors declare no conflict of interests.

Bibliography

Ackermann, F. (1999). Airborne laser scanning - Present status and future expectations. *ISPRS Journal of Photogrammetry and Remote Sensing*, 54(2–3), 64–67. [https://doi.org/10.1016/S0924-2716\(99\)00009-X](https://doi.org/10.1016/S0924-2716(99)00009-X)

Beyer, H. L. (2012). Geospatial Modelling Environment. *Geospatial Modeling Environment*. <https://doi.org/http://www.spatial ecology.com/gme>

Bowler, D. E., Buyung-Ali, L., Knight, T. M., & Pullin, A. S. (2010). Urban greening to cool towns and cities: A systematic review of the empirical evidence. *Landscape and Urban Planning*, 97(3), 147–155. <https://doi.org/10.1016/j.landurbplan.2010.05.006>

Breadboard Labs. (2018). *Measurement & spatial analysis of London 's tree canopy cover: 2018 methodology report*.

Chen, Q., Baldocchi, D., Gong, P., & Kelly, M. (2006). Isolating individual trees in a savanna woodland using small footprint lidar data. *Photogrammetric Engineering and Remote Sensing*, 72(8), 923–932. <https://doi.org/10.14358/PERS.72.8.923>

Demir, N., Poli, D., & Baltsavias, E. (2008). Extraction of buildings and trees using images and LIDAR data: *International Archives of the Photogrammetry, Remote Sensing and Spatial Information Sciences*, 37(B4), 313–318. <https://doi.org/Export Date 6 May 2013>

ESA. (n.d.). Curio Canopy Urban forest community platform | ESA Business Applications. Retrieved June 13, 2019, from <https://business.esa.int/projects/curio-canopy>

Haaland, C., & van den Bosch, C. K. (2015). Challenges and strategies for urban green-space planning in cities undergoing densification: A review. *Urban Forestry and Urban Greening*, 14(4), 760–771. <https://doi.org/10.1016/j.ufug.2015.07.009>

McPherson, E. G., & Kendall, A. (2014). A life cycle carbon dioxide inventory of the Million Trees Los Angeles program. *International Journal of Life Cycle Assessment*, 19(9), 1653–1665. <https://doi.org/10.1007/s11367-014-0772-8>



Perko, R., Raggam, H., Gutjahr, K. H., & Schardt, M. (2015). Advanced DTM generation from very high resolution satellite stereo images. *ISPRS Annals of the Photogrammetry, Remote Sensing and Spatial Information Sciences*, 2(3W4), 165–172. <https://doi.org/10.5194/isprsannals-II-3-W4-165-2015>

Planet Labs. (2018). *Planet imagery product specifications*. Retrieved from https://assets.planet.com/docs/Planet_Combined_Imagery_Product_Specs_letter_screen.pdf

Poli, D., & Caravaggi, I. (2012). *Digital surface modelling and 3D information extraction from spaceborne very high resolution stereo pairs: photogrammetric processing of stereo imagery over large metropolitan areas for global security and crisis management*. <https://doi.org/10.2788/15526>

Ratti, C., Seiferling, I., Li, X., Ghaeli, N., & So, W. (n.d.). Treepedia - MIT Senseable City Lab. Retrieved June 13, 2019, from <http://senseable.mit.edu/treepedia>

Rouse, J., Haas, R., Deering, D., Schell, J., & Harlan, J. (1974). *Monitoring the Vernal Advancement and Retrogradation (Green Wave Effect) of Natural Vegetation*. Washington, DC, United States.

Sohn, G., & Dowman, I. (2007). Data fusion of high-resolution satellite imagery and LiDAR data for automatic building extraction. *ISPRS Journal of Photogrammetry and Remote Sensing*, 62(1), 43–63. <https://doi.org/10.1016/j.isprsjprs.2007.01.001>

Straub, B. (2004). A Multiscale Approach for the Automatic Extraction of Tree Tops. *Proceedings of the XXth ISPRS Congress Geo-Imagery Bridging Continents*. Istanbul: Commission III, WG (Vol. 4).

Vauhkonen, J., Ene, L., Gupta, S., Heinzl, J., Holmgren, J., Pitkänen, J., ... Maltamo, M. (2012). Comparative testing of single-tree detection algorithms under different types of forest. *Forestry*, 85(1), 27–40. <https://doi.org/10.1093/forestry/cpr051>

Weier, J., & Herring, D. (2000). Measuring Vegetation (NDVI & EVI).